

Precision of sustained fixation in trained and untrained observers

Claudia Cherici

Department of Psychology, Boston University,
Boston, MA, USA



Xutao Kuang

Department of Psychology, Boston University,
Boston, MA, USA



Martina Poletti

Department of Psychology, Boston University,
Boston, MA, USA



Michele Rucci

Department of Psychology and Graduate Program in
Neuroscience, Boston University, Boston, MA, USA



During visual fixation, microscopic eye movements shift the image on the retina over a large number of photoreceptors. Although these movements have been investigated for almost a century, the amount of retinal image motion they create remains unclear. Currently available estimates rely on assumptions about the probability distributions of eye movements that have never been tested. Furthermore, these estimates were based on data collected with only a few, highly experienced and motivated observers and may not be representative of the instability of naive and inexperienced subjects in experiments that require steady fixation. In this study, we used a high-resolution eye-tracker to estimate the probability distributions of gaze position in a relatively large group of human observers, most of whom were untrained, while they were asked to maintain fixation at the center of a uniform field in the presence/absence of a fixation marker. In all subjects, the probability distribution of gaze position deviated from normality, the underlying assumption of most previous studies. The resulting fixational dispersion of gaze was much larger than previously reported and varied greatly across individuals. Unexpectedly, the precision by which different observers maintained fixation on the marker was best predicted by the properties of ocular drift rather than those of microsaccades. Our results show that, during fixation, the eyes move by larger amounts and at higher speeds than commonly assumed and highlight the importance of ocular drift in maintaining accurate fixation.

Keywords: fixational eye movements, ocular drift, saccade, microsaccade, fixation accuracy

Citation: Cherici, C., Kuang, X., Poletti, M., & Rucci, M. (2012). Precision of sustained fixation in trained and untrained observers. *Journal of Vision*, 12(6):31, 1–16, <http://www.journalofvision.org/content/12/6/31>, doi:10.1167/12.6.31.

Introduction

During fixation on a stationary object, slow drifts and small saccades (known as microsaccades or fixational saccades) continually shift the line of sight. These microscopic movements have attracted considerable interest because of their possible roles in visual acuity (Ahissar & Arieli, 2001; Averill & Weymouth, 1925; Marshall & Talbot, 1942), the prevention of image fading (Collewijn & Kowler, 2008; Ditchburn & Ginsborg, 1952; Martinez-Conde et al., 2006; Riggs & Ratliff, 1952; Yarbus, 1967), and, more recently, the relocation of attention (Engbert & Kliegl, 2003; Hafed & Clark, 2002;), and the perception of fine spatial detail (Ko et al., 2010; Rucci et al., 2007).

Despite this long interest, the precision by which human observers maintain fixation and the relative contributions of microsaccades and drift to the dispersion of gaze have remained unclear. Previous studies that examined the area covered by fixational instability have reported relatively small dispersions of gaze during fixation on a marker (Bennet-Clark, 1964; Boyce, 1967; Ditchburn, 1973; Fiorentini & Ercoles, 1966; Krauskopf et al., 1960; Nachmias, 1959; Rattle, 1969; Sansbury et al., 1973; Skavenski et al., 1979; Skavenski & Steinman, 1970; Steinman, 1965). However, these estimates were derived from measurements of eye movements in very few subjects, typically the experimenters themselves and/or observers with extensive experience with experiments that required prolonged and accurate fixation. Furthermore, these studies did not attempt to reconstruct the 2D proba-

bility distribution of gaze position during fixation. They directly estimated its area on the basis of specific assumptions (usually joint normality), which have never been tested. Therefore, while it is known that highly trained and motivated observers are capable of maintaining very accurate fixation for prolonged periods of time, a systematic analysis of the fixational distribution of gaze position and its underlying oculomotor factors in a population of inexperienced observers is currently not available in the literature.

This gap has resulted primarily from the limitations of eye-tracking methods. Older methods, such as the optical lever technique and the use of eye coils in magnetic fields, possess spatial and temporal resolutions, which are well suited for the analysis of microscopic eye movements. However, because of their invasiveness, these methods do not lend themselves to the analysis of large populations of observers. They also give a limited temporal window of observation, making it difficult to acquire the large volume of data necessary to estimate the probability distribution of gaze position. In contrast, the flexibility and usability of modern video-based eye-trackers are ideal for examining large pools of subjects for prolonged periods of time. But it remains unclear whether these systems possess sufficient resolution for detecting the microscopic eye rotations resulting from the smallest microsaccades and ocular drift.

This study has two main goals. The first goal is to estimate the precision of fixation in a sizeable population of naive and inexperienced observers when they are asked to maintain their gaze steady on a marker or at a given location of the display. Sustained fixation remains a frequent requirement in vision research experiments, but the classical measurements obtained with highly trained and motivated observers may not accurately describe the fixational behavior of the broader pools of subjects of modern experiments. The second goal is to link individual differences in the characteristics of ocular drift and microsaccades to the precision of fixation of different observers. Although idiosyncratic differences have long been known to exist in the patterns of microscopic eye movements, a systematic analysis of this variability has not been reported in the literature.

To overcome the limitations of previous studies, we record eye movements by means of a Dual Purkinje Image eye-tracker (Fourward Technologies, Gallatin, MO) (Crane & Steele, 1985)—a minimally invasive system that provides an excellent trade-off between resolution and flexibility—and estimate the probability density function of fixational gaze position. This approach allows rigorous evaluation of the area covered by fixational instability without relying on arbitrary assumptions about the shape of the distribution, as in previous studies. We show that during

sustained fixation, microscopic eye movements move the eyes by larger amount than commonly believed.

Methods

Subjects

A total of 14 observers with normal, non-corrected vision participated in the study (age range: 20–40 years). All observers, with the exception of one of the authors (CC), were naive about the purposes of the experiment. Three of them (subjects CC, WW, DR) had previous experience with psychophysical experiments requiring prolonged fixation (trained group). The remaining 11 had never participated in a vision research experiment before (untrained group). Informed consent was obtained from all participants following the procedure approved by the Boston University Charles River Campus Institutional Review Board.

Apparatus and stimuli

The experiments were conducted in a dimly illuminated room. Stimuli were displayed on a fast phosphor monitor (Iyamaya HM204DT) at a resolution of 800×600 pixels and vertical refresh rate of 200 Hz. Subjects were kept at a fixed distance of 125 cm from the monitor. A dental imprint bite bar and a head rest prevented movements of the head. The movements of the right eye were measured by means of a Generation 6 Dual Purkinje Image (DPI) eyetracker (Fourward Technologies). The internal noise of this system is about $20''$ (Crane & Steele, 1985), enabling a spatial resolution of eye movement of approximately $1'$ (Stevenson and Roorda, 2005). Vertical and horizontal eye positions were sampled at 1 kHz and recorded for subsequent analysis. Stimuli were observed monocularly, with the left eye patched. This was necessary because we only measured movements of the right eye and used a gaze-contingent calibration procedure to improve localization of the line of sight (see Procedure).

Procedure

Observers were asked to maintain accurate fixation for 5 s either in the presence (marker condition) or in the absence (no-marker condition) of a fixational marker, a $4'$ dot displayed at maximum contrast at the center of the monitor on a uniformly black background. Data were collected in separate experi-

mental sessions, each of approximately 1-hour duration. Every session started with preliminary setup operations that lasted a few minutes and allowed the subject to adapt to the low level of light in the room. Preliminary operations included: (1) positioning the subject optimally and comfortably in the apparatus; (2) tuning the eyetracker; and (3) performing a calibration procedure to convert the voltages given by the eyetracker into degrees of visual angle. These operations were repeated before each block of trials within each session.

The calibration procedure consisted of two phases. In the first phase (automatic calibration), subjects sequentially fixated on each of the nine points of a 3×3 grid, as it is standard in oculomotor experiments. In the second phase (manual calibration), subjects confirmed or refined the voltage-to-pixel mapping given by the automatic calibration. In this phase, they fixated again on each of the nine points of the grid, while the location of the line of sight estimated on the basis of the automatic calibration was displayed in real time on the screen. Subjects used a joystick to correct its position, if necessary. These corrections were then incorporated into the voltage-to-pixel transformation. This dual-step calibration allows more accurate localization of gaze position than a standard single-step procedure (Ko et al., 2010). Subjects were then presented with four blocks of 20 experimental trials. Breaks between consecutive blocks ensured that subjects were never constrained in the apparatus for more than 10 to 15 minutes consecutively.

Data analysis

Recorded eye movements traces were segmented into separate periods of drift and saccades. Classification of eye movements was performed automatically and then validated by human experts. Periods of blinks were automatically detected by the DPI eye-tracker and removed from data analysis. Only trials with optimal, uninterrupted tracking, in which the fourth Purkinje image was never eclipsed by the pupil margin, were selected for data analysis.

Eye movements with minimal amplitude of $3'$ and peak velocity higher than $3^\circ/s$ were selected as possible saccadic events. Consecutive events closer than 15 ms were merged together into a single saccade, a method, which automatically excluded post-saccadic overshoots. These transients result from the movement of the lens and, possibly, the damping of the eye-tracker (Deubel & Bridgeman, 1995; Stevenson & Roorda, 2005). Saccade amplitude was defined as the modulus of the vector connecting the two locations at which eye speed became greater (saccade onset) and lower

(saccade offset) than $2^\circ/s$. Saccadic rates were calculated over the entire duration of each trial. In this study, we do not distinguish between saccades and microsaccades; all saccadic movements are analyzed together independent of their magnitudes. Periods that were not classified as saccades or blinks were automatically labeled as drifts.

The overall precision of fixation was measured by means of the fixation span, defined as the area around the mean gaze position, which contained the line of sight with a desired probability \hat{p} . For each subject, in every experimental condition, we first estimated the 2D probability density function of eye position, $f(x,y)$, by pooling together all the available trials and estimating 2D histograms on a grid with bin size $1.2' \times 1.2'$. The size of the grid was adjusted for each subject to cover the entire area of fixation. To eliminate possible calibration offsets, traces from different trials were aligned by subtracting their mean positions. We then estimated the value c yielding the region $S_c = \{(x,y) : f(x,y) \geq c\}$ in which the line of sight was found with probability \hat{p} :

$$\iint_{S_c} f(x,y) dx dy = \hat{p}$$

The fixation span was defined as the area of S_c . This method is equivalent to finding the region corresponding to the $(100 \cdot \hat{p})$ th percentile of the distribution of gaze position. Unless otherwise indicated, data refer to the area with $\hat{p} = 0.75$ probability. That is, the fixation span indicates the area of the region around the mean position in which the line of sight was found 75% of the time.

Probability density maps of saccades and drift velocity were estimated (in polar coordinates) following a procedure similar to that used for position signals. To limit the impact of noise, the intersaccadic periods of drift were low-pass filtered by means of a third-order Savitzky-Golay filter over 41 samples (Figure 1). This method performs a local polynomial regression and was preferred over more traditional filters because of its higher stability during the initial and final intervals of each drift segment (Savitzky & Golay, 1964). Velocity signals were calculated as the temporal derivatives of the filtered eye position traces. The speed of ocular drift indicates the modulus of the instantaneous velocity vector. To estimate the degree by which a drift episode differed from linear motion, we defined an index of curvature, $IC = 1 - (\text{drift amplitude}/\text{drift length})$. The amplitude of a drift period was defined as the modulus of the vector connecting its initial and final positions, and its length as the arc length of the intersaccadic trajectory. $IC = 1$ represents a period of drift which starts and ends at the same point. $IC = 0$ indicates a drift period with linear motion characteristics.

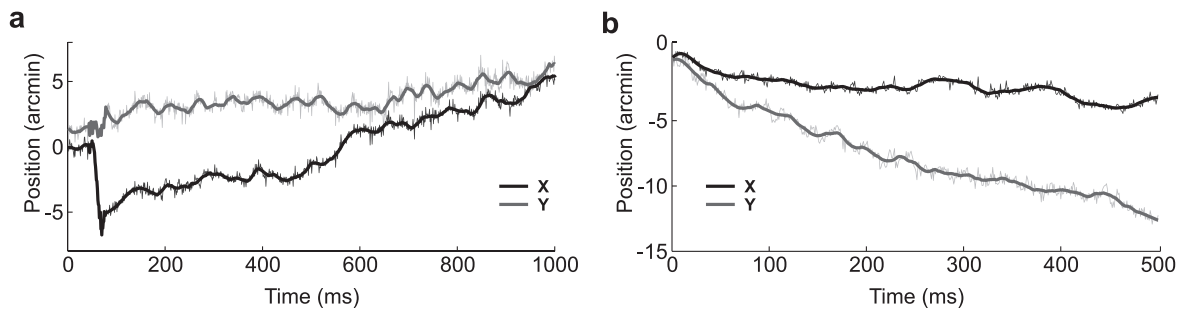


Figure 1. Examples of the raw eye movement data recorded in the experiments (thin lines) and filtered traces (thick lines). The two curves in each panel represent horizontal and vertical eye movements. The two panels show traces from the most accurate (subject WW; left) and the least accurate (subject DG; right) observers in our pool.

The shape of all probability density functions were quantified by means of two parameters: the angle of the principal axis of the distribution (θ) and the index of symmetry (SI). Both parameters were obtained by means of principal component analysis of the horizontal and vertical pairs used to estimate the density maps. θ was defined as the angle of the eigenvector associated with the largest eigenvalue. An angle $\theta = 0$ indicates a horizontal axis. The index of symmetry was defined as $\sqrt{\lambda_2/\lambda_1}$, where λ_1 and λ_2 are the two eigenvalues ($\lambda_1 \geq \lambda_2$). $SI = 1$ represents a circular distribution.

To quantify individual differences in oculomotor strategies, for each subject, we estimated how the area of fixation in a single trial varied as a function of the considered oculomotor parameters. For each subject, in every available trial t , we measured the area of the 68th confidence ellipse, E_t , together with the values of the four oculomotor variables: saccadic rate (R_t),

saccadic amplitude (A_t), drift speed (S_t) and drift curvature (C_t). The resulting distributions of the four variables were then normalized by removing their means and dividing by their standard deviations, so that the corresponding regression weights could be directly compared. We then fitted, by means of least-squares, the linear model:

$$E_t = w_0 + w_1 \tilde{R}_t + w_2 \tilde{A}_t + w_3 \tilde{S}_t + w_4 \tilde{C}_t$$

where the tilde indicates normalization of the corresponding measurement. Table 4 reports the coefficients w_1 - w_4 obtained from this multiple regression together with the accuracy of the fit.

As a rough measurement of the interplay between the angles of saccades and drifts, we examined in which direction (α_1) an oculomotor event (saccade, drift period) moved the line of sight relative to the direction (α_0) of the event which preceded it (drift period, saccade). We first calculated the distribution of the angular difference $\Delta\alpha = \alpha_1 - \alpha_0$ between two successive oculomotor events (Figure 5a-d). For each distribution, we then computed a compensation index as the difference between the proportions of consecutive events moving in similar ($|\Delta\alpha| < 45^\circ$) and opposite ($|\Delta\alpha - 180^\circ| < 45^\circ$) directions (Figure 5e).

Subject	Marker condition			No marker condition		
	Fix. Span	θ	SI	Fix. Span	θ	SI
WW*	71	26	0.48	305	4	0.27
DR*	127	133	0.45	881	99	0.78
CM	177	114	0.65	514	97	0.29
FP	184	40	0.76	1706	23	0.62
CC*	199	1	0.33	1132	177	0.20
NF	238	161	0.47	1178	169	0.30
CK	255	22	0.60	736	172	0.53
TL	340	32	0.66	1477	177	0.48
EF	386	178	0.70	1473	160	0.62
EW	405	38	0.47	1584	139	0.76
LR	521	179	0.86	1479	3	0.20
MG	592	5	0.20	2370	9	0.48
DK	645	9	0.31	1621	8	0.30
DG	994	32	0.68	1472	23	0.49

Table 1. Individual gaze position data. Columns represent (from left to right): the fixation span (arcmin²); the angle of the principal axis (degree); and the index of symmetry. Corresponding probability maps are shown in Figure 2. Asterisks mark the experienced observers.

Results

To quantify the precision by which humans maintain prolonged fixation, we estimated the probability density function of gaze position in 14 observers, 11 of whom had no previous experience with experiments requiring sustained fixation (untrained group). Subjects were instructed to fixate as accurately as possible at the center of a cathode ray tube (CRT) display in the presence or in the absence of a fixation marker (marker and no-marker conditions, respectively). In both conditions, the edges of the monitor were clearly visible.

Subject	Marker condition				No marker condition			
	Amp.	Rate	θ	SI	Amp.	Rate	θ	SI
WW*	8 ± 4	1.26 ± 0.49	29	0.28	17 ± 11	0.95 ± 0.42	15	0.32
DR*	12 ± 6	0.44 ± 0.36	176	0.16	27 ± 13	0.90 ± 0.48	158	0.52
CM	16 ± 11	0.81 ± 0.45	166	0.44	34 ± 14	0.16 ± 0.24	159	0.57
FP	13 ± 7	1.83 ± 0.49	101	0.60	51 ± 29	1.28 ± 0.52	8	0.52
CC*	30 ± 14	0.73 ± 0.52	178	0.14	67 ± 21	0.82 ± 0.51	179	0.09
NF	24 ± 8	0.98 ± 0.54	156	0.53	57 ± 21	0.64 ± 0.52	170	0.25
CK	15 ± 8	1.48 ± 0.67	47	0.87	25 ± 15	0.79 ± 0.62	19	0.41
TL	17 ± 9	1.54 ± 0.93	9	0.53	40 ± 24	1.71 ± 0.89	179	0.38
EF	19 ± 9	1.77 ± 0.93	0	0.33	34 ± 17	1.37 ± 0.76	178	0.41
EW	19 ± 15	0.98 ± 0.44	107	0.48	38 ± 20	0.66 ± 0.42	165	0.13
LR	19 ± 9	2.29 ± 1.19	171	0.41	32 ± 17	2.14 ± 1.21	5	0.37
MG	31 ± 12	1.42 ± 0.66	179	0.08	60 ± 19	1.12 ± 0.63	179	0.08
DK	30 ± 12	1.43 ± 0.70	3	0.27	47 ± 20	1.22 ± 0.79	4	0.21
DG	22 ± 14	1.59 ± 0.91	2	0.26	34 ± 18	1.21 ± 0.77	179	0.16

Table 2. Individual saccade data. Notes: Columns represent (from left to right): mean and standard deviation of the saccade amplitude (arcmin); mean and standard deviation of the saccade rate (saccades per second); the angle of the principal axis (degree); and the index of symmetry. Corresponding probability maps are shown in Figure 3.

Figure 2 shows the probability density function of gaze position for each individual observer. The parameters describing these distributions are reported in Table 1. In the marker condition, the span of fixation—the area containing the line of sight with 0.75 probability—had a mean of 367 arcmin² and a standard deviation of 251 arcmin² (Figure 2a). The average span of the untrained group was more than three times larger than the span of the experienced observers (trained group: 132 arcmin²; untrained group: 431 arcmin²; $p = 0.065$, unpaired t-test). The fixation span varied across subjects by a factor of 14: the value for the most stable subject (WW, a trained observer) was 71 arcmin², while the least stable subject

(DG) had a value of 994 arcmin². Several observers exhibited roughly circular probability distributions, as quantified by the symmetry index (SI) in Table 1 (SI close to 1). Radial symmetry was particularly pronounced in observers FP and LR. However, in a considerable group of subjects the distribution of gaze position was more elliptical, an effect which was evident in subjects MG and DK. For this latter group of subjects, the primary axis of dispersion of gaze position also varied; it was horizontal (θ close to 0°) in several (CC, MG, and DK), but not all observers (e.g., DR, CM).

Figure 2b shows the dispersion of gaze measured in the same subjects when they maintained fixation at the

Subject	Marker condition				No marker condition			
	Speed	Curv. Ind	θ	SI	Speed	Curv. Ind	θ	SI
WW*	44 ± 35	0.79 ± 0.18	74	0.42	44 ± 29	0.78 ± 0.19	73	0.44
DR*	30 ± 17	0.69 ± 0.20	-105	0.62	37 ± 23	0.52 ± 0.18	-82	0.52
CM	37 ± 22	0.70 ± 0.22	-122	0.51	37 ± 21	0.73 ± 0.14	71	0.55
FP	38 ± 26	0.64 ± 0.17	-110	0.57	40 ± 28	0.50 ± 0.18	-95	0.46
CC*	45 ± 28	0.71 ± 0.23	-104	0.59	46 ± 27	0.62 ± 0.19	-85	0.65
NF	40 ± 27	0.54 ± 0.22	-91	0.58	42 ± 26	0.47 ± 0.21	-54	0.73
CK	61 ± 39	0.69 ± 0.21	78	0.35	62 ± 42	0.69 ± 0.23	71	0.38
TL	50 ± 50	0.60 ± 0.20	-118	0.49	50 ± 31	0.51 ± 0.21	-138	0.52
EF	51 ± 55	0.54 ± 0.23	-97	0.60	65 ± 71	0.52 ± 0.23	61	0.51
EW	61 ± 39	0.74 ± 0.20	89	0.56	66 ± 43	0.67 ± 0.16	91	0.46
LR	86 ± 93	0.65 ± 0.22	-103	0.40	112 ± 116	0.62 ± 0.21	-98	0.34
MG	49 ± 30	0.63 ± 0.21	-107	0.66	58 ± 58	0.50 ± 0.22	-97	0.51
DK	49 ± 33	0.47 ± 0.19	-107	0.42	55 ± 38	0.36 ± 0.20	-104	0.34
DG	89 ± 63	0.67 ± 0.23	-106	0.24	90 ± 64	0.65 ± 0.23	-107	0.23

Table 3. Individual ocular drift data. Notes: Columns represent (from left to right): means and standard deviations of speed (arcmin/s), and index of curvature; angle of the principal axis (deg); index of symmetry. Corresponding probability maps are shown in Figure 4.

Subject	Marker condition					No marker condition				
	Rate	Amp.	Speed	Curv.	R ²	Rate	Amp.	Speed	Curv.	R ²
WW*	0.01	0.09	0.32	−0.07	0.35	0.22	0.30	0.45	−0.01	0.52
DR*	0.15	0.30	0.25	0.02	0.32	0.21	0.68	0.15	−0.15	0.56
CM	0.14	0.15	0.01	−0.02	0.51	0.19	0.08	−0.01	−0.07	0.18
FP	0.23	0.46	0.06	0.03	0.59	0.42	0.38	0.34	0.08	0.36
CC*	0.20	0.38	0.34	−0.02	0.36	0.18	0.39	0.23	0.01	0.37
NF	0.19	0.46	0.30	0.09	0.70	0.65	0.25	0.23	−0.03	0.50
CK	0.22	0.37	0.16	−0.02	0.66	0.28	0.38	0.08	−0.21	0.54
TL	0.31	0.41	0.30	−0.17	0.38	0.40	0.41	0.16	−0.02	0.42
EF	0.09	0.13	0.39	−0.05	0.50	0.26	0.57	0.15	−0.21	0.38
EW	0.08	0.24	0.10	−0.03	0.56	0.01	0.37	0.26	−0.29	0.35
LR	0.09	0.10	0.47	−0.04	0.78	0.54	0.57	0.51	−0.07	0.49
MG	0.13	0.10	0.28	−0.38	0.37	0.02	0.17	0.20	−0.49	0.49
DK	−0.03	0.11	0.20	−0.17	0.62	0.09	0.42	0.43	−0.18	0.60
DG	0.04	0.09	0.23	−0.13	0.37	0.18	0.50	0.33	−0.08	0.53

Table 4. Regression and determination coefficients of a linear multiple regression model of fixation span. Notes: For each observer, the most influential oculomotor variable is marked in bold.

center of the monitor without a fixation marker. Fixation accuracy deteriorated drastically in this condition, yielding an average span of 1281 arcmin² ($p < 0.001$, paired t-test), a factor of 4 higher than the span measured in the presence of the marker. This deterioration in stability occurred for both experienced and inexperienced observers (average span trained group: 773 arcmin²; untrained group: 1419 arcmin²). However, the exact amount by which the fixation span increased varied substantially across observers, from a ratio of 1.45 in subject DG to 9 in subject FP. The resulting area ranged from a minimum of 305 arcmin² (subject WW) to a maximum of 2370 arcmin² (subject MG). This enlargement of the probability distribution of gaze position was not the result of a simple rescaling of the function measured during fixation on a marker. For three observers (DR, EW, MG), the gaze distribution became more circular, whereas it was more elongated for all the others. Stretching of the distribution along one axis was particularly evident for observers CC and LR. Even though the dispersion of gaze enlarged in a complex and idiosyncratic way during fixation on a uniform field, the precision of fixation in the two conditions (marker and no-marker) was highly correlated ($r = 0.6$, $p < 0.03$).

Figure 2c and d show the cumulative probability functions of gaze position (the probability that the line of sight was within a given area) averaged across all observers in each group. These graphs summarize the enlargement in the span of fixation caused by the removal of the marker. For comparison, Figure 2c and d also show the average area that would have been estimated in the untrained group using the traditional method of the confidence ellipse (Nachmias, 1959). Estimates obtained with this method differed substan-

tially from the direct measurements of the fixational area, an effect that was particularly pronounced in the no-marker condition. These differences occurred because the 2D distributions of gaze position deviated from normality. In both conditions, all marginal distributions on both the x and y axis were significantly different from normal distributions ($p < 0.001$; Jarque-Bera test).

Figure 3 and Table 2 show the characteristics of the saccades recorded in the experiments. During fixation on a marker, the mean rate across all observers was 1.32 saccades/s with a standard deviation of 0.5 saccades/s. Experienced observers performed less saccades than inexperienced ones (trained group: 0.81 saccades/s; untrained group: 1.47 saccades/s; $p < 0.04$, unpaired t-test). The mean saccadic amplitude was 20' with a standard deviation of 7', with little difference between the two groups (trained group: 17'; untrained group: 20'; $p = 0.43$, unpaired t-test). Saccade characteristics varied considerably across observers. The rate ranged from 0.44 saccades/s (subject DR) to 2.29 saccades/s (subject LR). Five observers executed less than one saccade per second (subjects DR, CM, CC, NF, and EW), and only one observer performed more than two saccades per second (subject LR). The average saccadic amplitude ranged from a minimum of 8' (subject WW) to a maximum of 31' (subject MG). As previously observed (Engbert & Kliegl, 2003), saccades were frequently on the horizontal axis (angle of the main axis of dispersion, θ , close to 0° or 180° in Table 2). However, saccades occurred in all directions, and the main axis of the distribution was tilted in several subjects (e.g., NF, CK, EW). The rate and amplitude of saccades were not correlated ($r = -0.02$, $p > 0.95$).

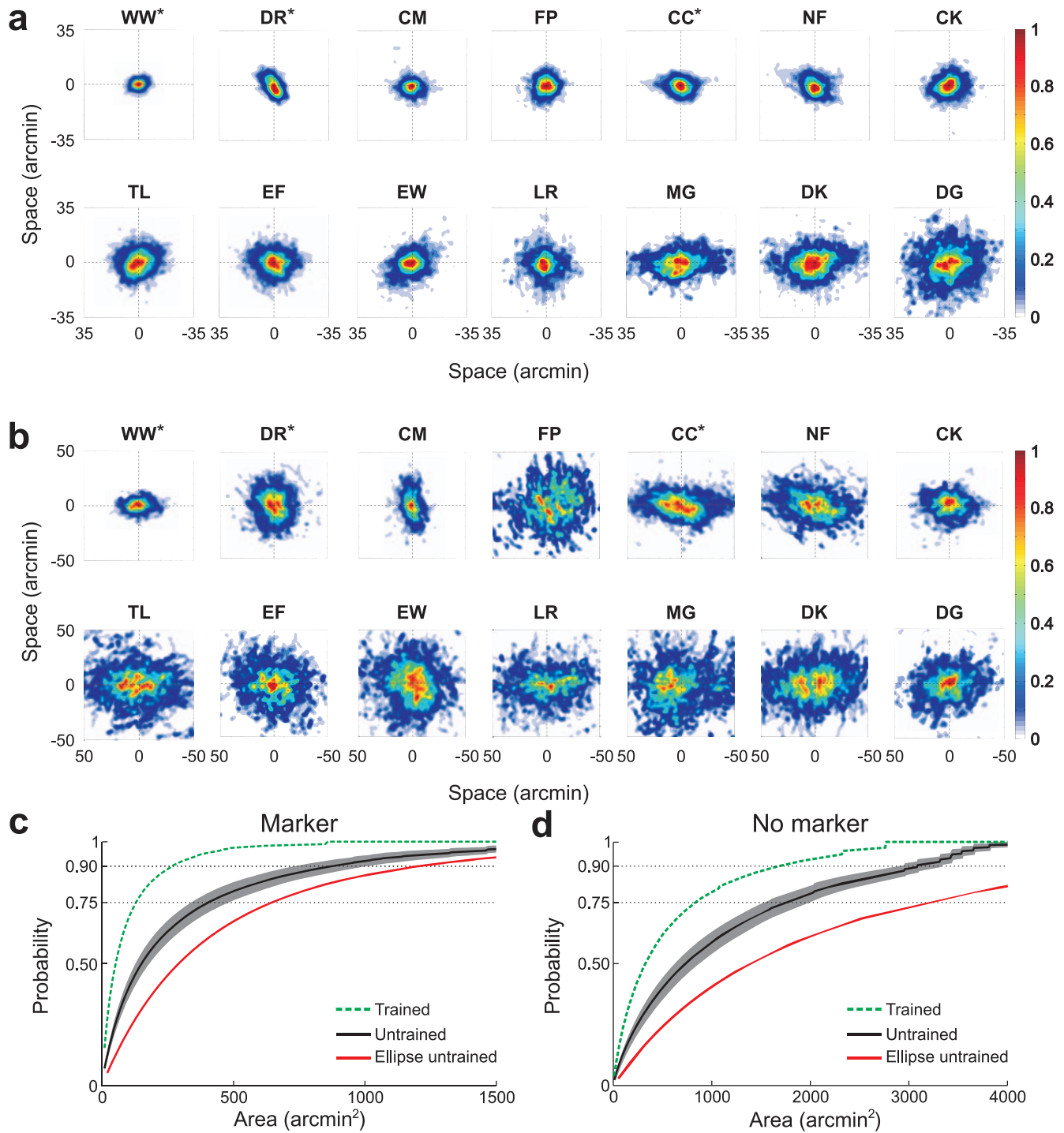


Figure 2. Precision of fixation. Probability density functions of gaze position for individual observers during sustained fixation on (a) a 4' dot (marker condition); and on (b) a uniform field (no-marker condition). Different panels refer to different subjects. Color codes the probability that the line of sight deviated by an amount corresponding to each pixel location. Distributions were normalized by their peak value for better visualization. Here and in the following Figures and Tables, asterisks mark the experienced observers. (c, d) Average cumulative probability across all the observers in the untrained group as a function of the span of fixation in the two experimental conditions (black). The shaded gray region represents *SEM*. For comparison, the average cumulative probability across trained observers (green) and the equivalent estimate given by the confidence ellipse (red) are also shown.

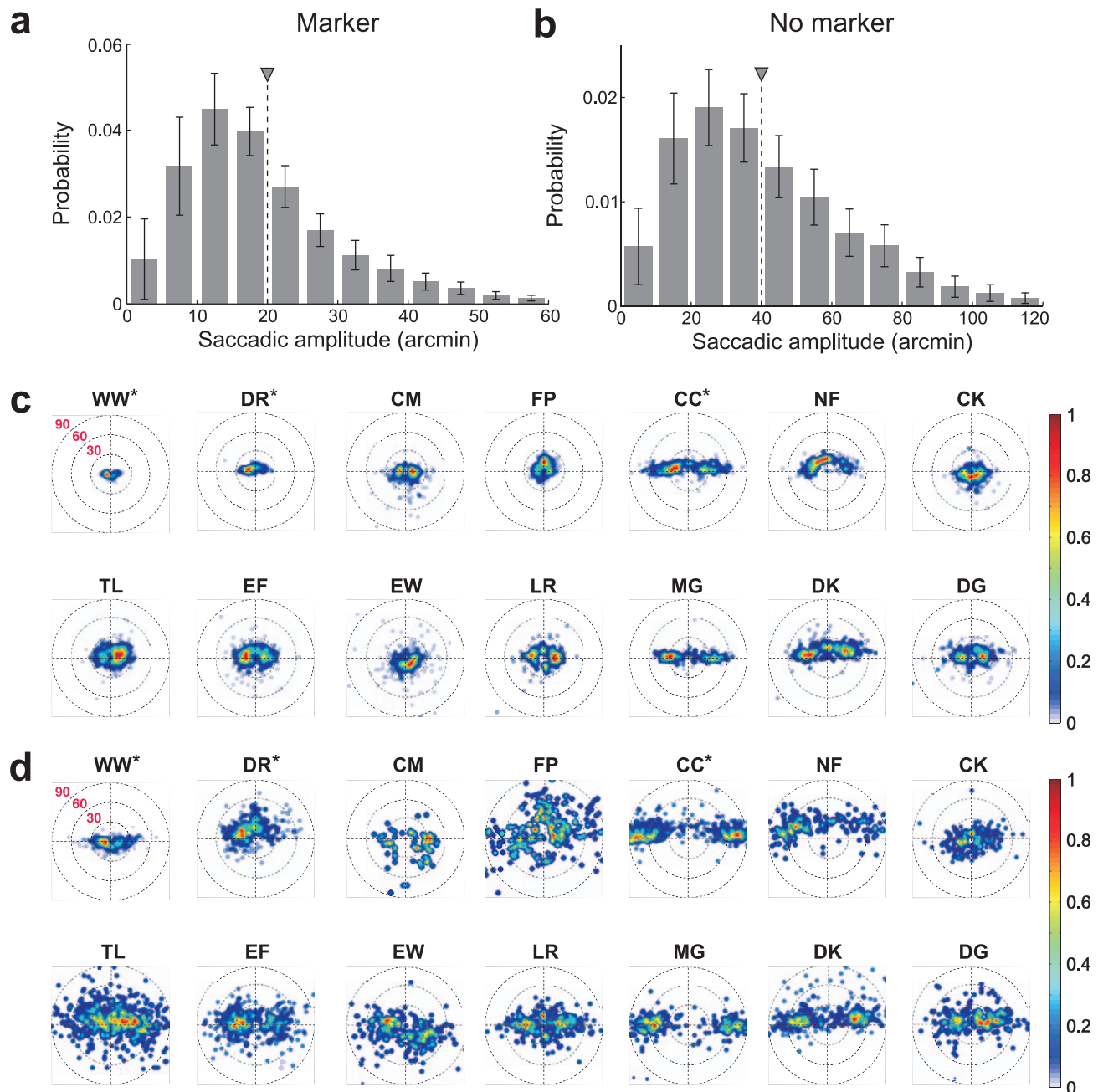


Figure 3. Characteristics of saccades. (a, b) Average probability distributions of saccadic amplitudes in the two experimental conditions. Data represent average \pm SEM of the amplitude distributions of individual subjects. Triangles indicate mean values. (c, d) Probability distributions of saccades for each individual observer during fixation on (c) a marker and (d) a uniform field.

Removal of the fixation marker affected saccades in two important ways (Figure 3b). First, in agreement with a previous study (Poletti & Rucci, 2010), the rate of saccades decreased significantly during fixation on a uniform field (mean rate: 1.07 saccades/s; $p < 0.05$, paired t-test), an effect almost exclusively caused by the inexperienced observers (mean rate untrained group: 1.12 saccades/s; $p < 0.005$). Seven out of 14 observers now executed less than one microsaccade per second. Second, the average amplitude of saccades increased in

every observer yielding a mean amplitude of 40' ($p < 0.005$, paired t-test) and now ranged from a minimum of 17' (subject WW) to a maximum of 67' (subject CC). The increment of saccadic amplitude was similar in the two groups of subjects (mean amplitude trained group: 37'; untrained group: 41'). On average across subjects, removal of the fixation marker, led to a much broader distribution of saccade amplitudes, with the 75th and the 95th percentiles equal to 51' and 75', respectively (Figure 3b). These modulations of both rate and

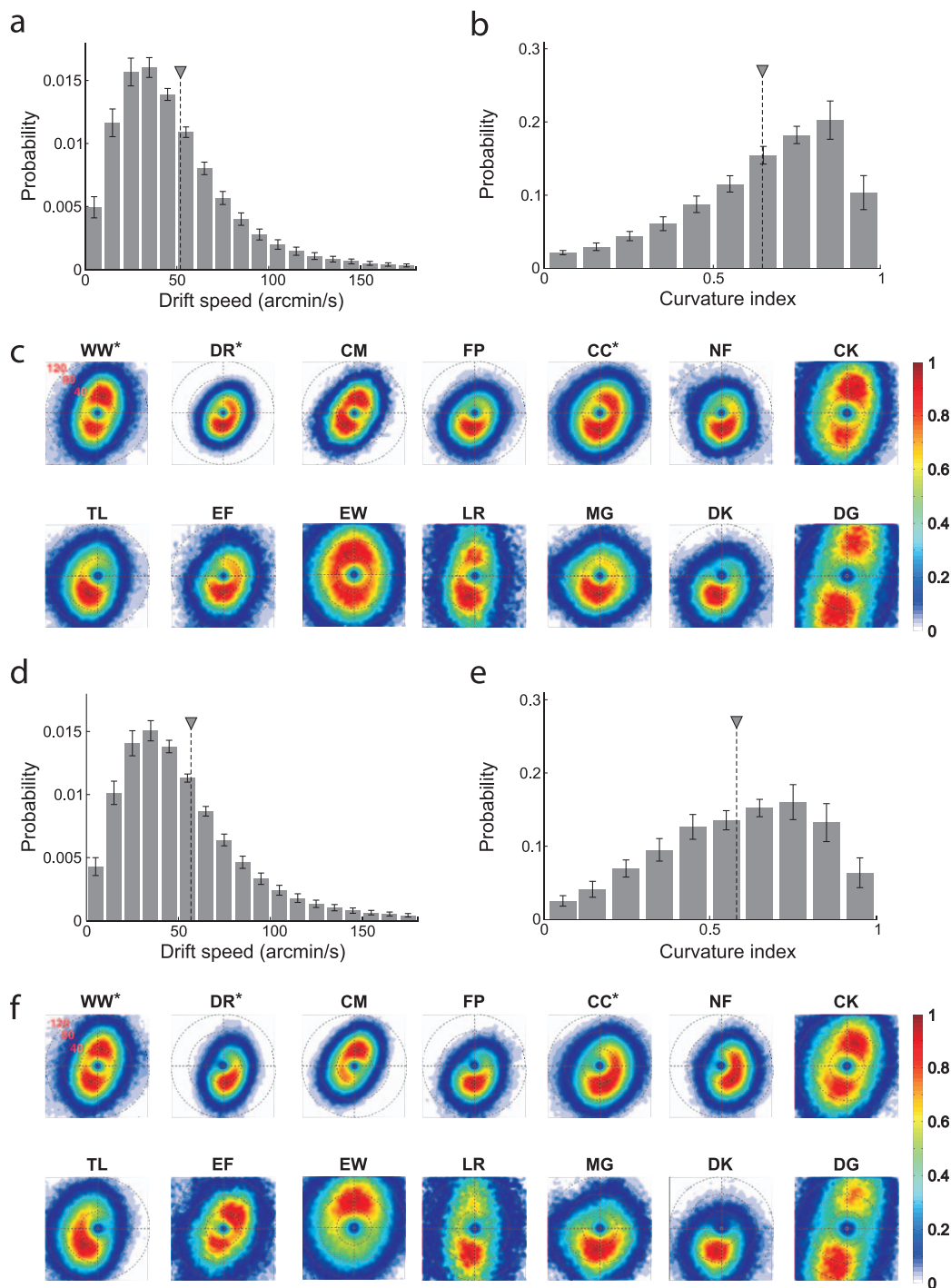


Figure 4. Characteristics of ocular drift. (a, b) Average probability distributions across all observers of (a) drift speed and (b) index of curvature in the marker condition. Error bars represent SEM. Triangles indicate mean values. (c) 2D probability distributions of instantaneous drift velocity for individual observers in the marker condition. Maps are in polar coordinates. Color codes the probability of occurrence of instantaneous drift velocity with given direction and modulus. (d-f) same as in (a-c) for the no-marker condition.

amplitude show that the visual feedback given by the presence of the fixation marker influenced the production of saccades. Interestingly, both amplitude ($r = 0.78$, $p = 0.001$) and rate ($r = 0.79$, $p < 0.005$) were highly correlated between the two conditions (marker and no-marker), indicating that observers with differ-

ent saccade characteristics were similarly affected by the removal of the fixation marker.

The characteristics of ocular drift were quantified by means of two parameters: instantaneous velocity and index of curvature (Figure 4 and Table 3; see Methods). During fixation on the marker, the instantaneous speed

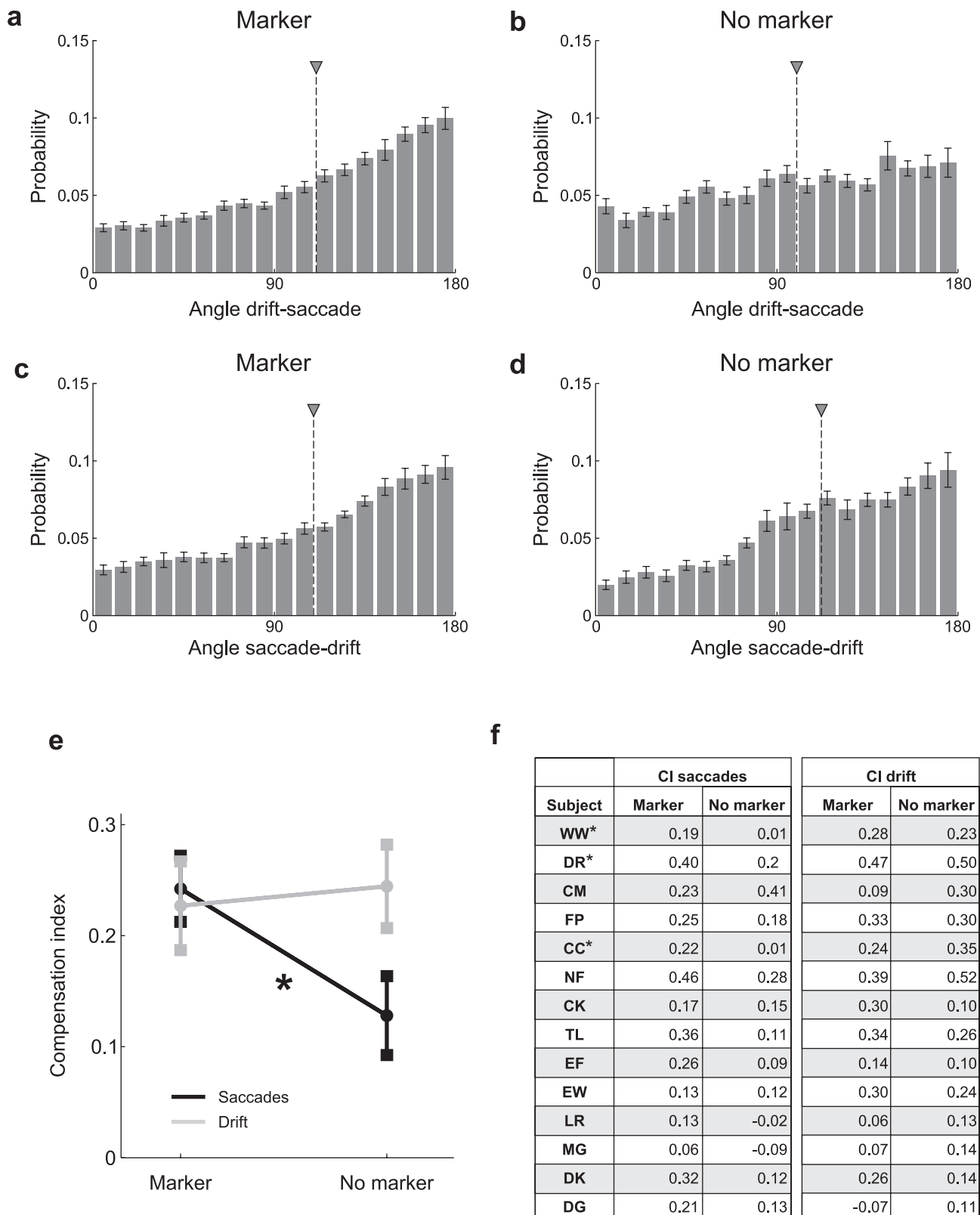


Figure 5. Interplay between saccades and drift. Average distributions across observers of the angular differences between consecutive oculomotor events: (a, b) angles of saccades relative to the preceding drifts, (c, d) angles of drifts relative to the preceding saccades. (e) Compensation indices in the two experimental conditions for saccades after drifts (saccades) and drifts after saccades (drift). Data represent means \pm SEM. (f) Compensation indices (CI) for individual observers.

of ocular drift (the modulus of the speed velocity vector, [Figure 4a](#)) was on average 52°/s and varied approximately by a factor of 3 across observers: from 30°/s for subject DR (a highly experienced subject) to 89°/s for subject DG. It was slightly higher for the inexperienced observers than for the experienced ones, a difference that did not reach statistical significance (mean instantaneous drift speed in the untrained group: 56°/s; trained group: 40°/s; $p = 0.16$, unpaired t-test). The actual 2D distributions of drift velocity differed substantially across observers ([Figure 4c](#)). Several subjects exhibited a downward vertical bias in the direction of drift (e.g., subjects FP, NF, DK, MG). Others, instead, possessed bidirectional (subjects WW, CK, DG) or almost circular (subjects EW, CC) distributions.

Drift episodes were highly curved with very few periods of unidirectional motion ([Figure 4b](#)). The average index of curvature was 0.65 and was again slightly higher in the trained group (untrained group average: 0.62; trained group: 0.73; $p = 0.056$, unpaired t-test). Also the index of curvature varied considerably across observers, ranging from 0.47 for subject DK to 0.79 for subject WW, another highly experienced observer. Drift speed and curvature were not correlated ($r = 0.05$; $p > 0.85$). However, these two parameters exhibited high correlations with saccade variables. The instantaneous drift speed was significantly correlated with the saccade rate ($r = 0.62$; $p < 0.02$), and the drift curvature possessed a negative correlation with the saccade amplitude, which was very close to significance ($r = -0.5$; $p = 0.066$). Thus, saccades were more frequent in subjects with faster drift and were larger in subjects with less self-compensatory drift.

[Figures 4d](#) through [f](#) show the characteristics of drift in the no-marker condition. Although changes were more subtle than for saccades, removal of the fixation marker also had a systematic influence on the characteristics of ocular drift. Both drift speed and index of curvature were very highly correlated in the marker and no-marker conditions (speed: $r = 0.95$, $p < 0.001$; curvature: $r = 0.87$, $p < 0.001$), showing that subjects maintained their individual drift characteristics. However, the average drift speed increased without a marker (mean speed: 57 ± 21 °/s; $p < 0.05$, paired t-test), an effect that was highly consistent across observers ([Figure 4d](#)). Furthermore, in almost all subjects, the directional distribution of drift velocity became more stretched in the absence of a marker ([Figure 4f](#)), so that a clear preferred direction now emerged even in the observers who did not exhibit a bias during fixation on the marker (e.g., subjects EW, CC). Drift was also less curved without the marker (mean curvature: 0.58 ± 0.12 ; $p < 0.05$, paired t-test. [Figure 4e](#)). These results are compatible with previous findings (Nachmias, 1961) and support the proposal

that drift is, at least in part, under active control of the oculomotor system (Steinman et al., 1973).

The data in [Figures 3](#) through [4](#) indicate that the maintenance of fixation is the result of a cooperation between ocular drift and saccades. This effect was particularly evident in subjects with a pronounced bias in the direction of ocular drift for whom saccades were often compensatory (e.g., DR, NF). To quantify this interaction, we examined the direction in which an oculomotor event (a microsaccade or a drift period) moved the line of sight relative to the event that immediately preceded it (a drift period or a microsaccade). During fixation on the marker, the distribution of angular differences between saccades and preceding periods of drift was significantly skewed toward 180° ([Figure 5a](#)). That is, saccades were significantly more likely to move the eye in the direction opposite to that of the preceding period of drift than in the same direction (mean compensation index: 0.24, $p < 0.05$). This effect was also present in the no-marker condition (mean compensation index: 0.13, $p < 0.05$; [Figure 5b](#)), but it was significantly less pronounced than during fixation on the marker ($p < 0.05$, paired t-test; [Figure 5e](#)).

As shown in [Figure 5c](#), in the marker condition, a period of drift was also more likely to move the eye in the direction opposite to that of the preceding saccade than in its same direction (mean compensation index: 0.23, $p < 0.05$). However, this effect was not influenced by the presence/absence of the fixation marker, and the angular distributions in the two conditions were very similar ([Figure 5d](#)). It should be noted that this effect was not caused by possible post-saccadic artifacts in the recordings, as results were virtually unaffected by excluding from data analysis the first 50 ms of each inter-saccadic segment. Thus, these data suggest that saccades and drifts tend to counteract each other during fixation.

The considerable intersubject variability in the data shown in [Figures 2](#) through [4](#) suggests that the precision of fixation of each observer was limited by their individual characteristics of eye movements. To better investigate this point, for each subject, we examined how the dispersion of gaze position in a single trial varied as a function of the four considered oculomotor variables (saccade rate, saccade amplitude, drift speed, and drift curvature; see [Methods](#)). The results in [Table 4](#) show that a multiple linear regression model was quite successful in predicting the area of fixational instability across trials. In the marker condition, the dispersion of gaze was primarily determined by the characteristics of saccades in eight subjects, and by the characteristics of drift in the remaining six. These changes in the weight allocation to the four oculomotor variables confirm that the relative contributions of drift and saccades varied across

subjects. In the no-marker condition, the characteristics of saccades were most influential in determining the span of fixation in all observers but two. Thus, saccades contributed more to the dispersion of gaze in the absence of the fixational marker than in its presence, suggesting again that saccades were less accurate without a clear fixation target.

Finally, we examined which oculomotor parameter better predicted the precision of fixation across observers. To this end, we estimated the amount of variance in the fixation span explained by linear regression with each of the four considered oculomotor variables. In the marker condition, only the speed of ocular drift yielded a significant regression. This variable gave a good fit of the fixation span ($r^2 = 0.56$; $p < 0.002$. Figure 6a through d). That is, observers with faster drifts were also less accurate in maintaining fixation. The mean amplitude of saccades was also close to significance, but accounted for a substantially lower portion of the variance. Results differed in the absence of the fixation marker, a condition in which drift speed was no longer significantly correlated with the span of fixation (Figure 6e through h). In this condition, two other variables became relevant: saccadic amplitude and drift curvature. These two variables were strongly anti-correlated ($r = -0.53$, $p < 0.05$), and both of them gave good fits of the fixation span, particularly drift curvature. Thus, knowledge of drift characteristics was a good predictor of the accuracy of fixation across observers also in the no-marker condition.

Discussion

Existing measurements of the precision of sustained fixation are based on data from highly experienced and motivated observers and rely on untested assumptions about the underlying distributions of gaze position. These measurements provide an estimate of the fixational stability that humans can reach, but tell us little about the actual oculomotor behavior of inexperienced and naive subjects in experiments that require fixation. In addition, little is known about the influences of the individual characteristics of eye movements on fixational stability. Yet fixational eye movements vary considerably across individuals. In this study, we examined fundamental oculomotor variables together with inter- and intra-subject variability in the precision of fixation in a significant population of inexperienced observers. This analysis has led to multiple findings, which are here analyzed in the context of current knowledge.

Our results show that human observers are less accurate in maintaining prolonged fixation than is

commonly believed. During fixation on a marker, the 95th percentile in the distribution of gaze was on average 967 arcmin^2 , an area equivalent to that of a $18'$ -radius circle. Without the marker, this area increased to 2801 arcmin^2 , a $30'$ -radius circle. The 68th percentiles were 275 arcmin^2 (marker) and 1113 arcmin^2 (no marker). These numbers are considerably larger than previously reported estimates in the literature, which ranged from 14 arcmin^2 (Ditchburn, 1973) to 244 arcmin^2 (Skavenski & Steinman, 1970). A survey of many early studies (Table 4.3 in Ditchburn [1973]; Sansbury et al. [1973]; Skavenski & Steinman [1970]; Skavenski et al. [1979]) gives an average 68th percentile of the fixation area equal to $73 \pm 50 \text{ arcmin}^2$, a value significantly lower than that estimated in our experiments ($p < 0.00001$; unpaired t -test). Interestingly, the two subjects with smallest dispersion of gaze in our experiments were two of the three experienced participants in our study. The fixation spans of these two experienced observers were within the ranges of previously reported data. Thus, our results suggest that experience and motivation play an important role in the pattern of fixational eye movements, and that previous estimates in the literature may have been biased by using a selected pool of highly trained subjects. Vision scientists should be careful in relying on these previous estimates, as they seriously underestimate the retinal image motion of untrained observers in experiments that require sustained fixation.

Our data also show that the assumption of normality of the distribution of gaze position, which was common to most previous studies, does not hold. In all subjects and all conditions, the marginal probability distributions on the two axes significantly deviated from normality. Since normality of the marginal distributions is a necessary condition for joint normality, the resulting 2D probability distributions significantly deviated from bivariate normal functions. Most previous studies implicitly assumed normality by calculating the fixation span by means of confidence ellipsoids (Nachmias, 1961; Steinman, 1965). To circumvent this problem, in this study, we directly estimated the probability distributions of gaze position. Similar attempts have been made by previous studies (Bennet-Clark, 1964; Boyce, 1967), but suffered from severe technological limitations. Interestingly, use of confidence ellipsoids in our data would have actually led to an even larger estimate of the fixation span, with a 68th percentile of 483 arcmin^2 in the marker condition.

Another important outcome of our study is the finding that, in the intersaccadic periods, the eyes move much faster than commonly appreciated: our estimate of the average drift speed is approximately one order of magnitude larger than previous values reported in the literature (typically $4'/\text{s}$; see Ditchburn [1973]). There are at least two reasons why commonly reported values

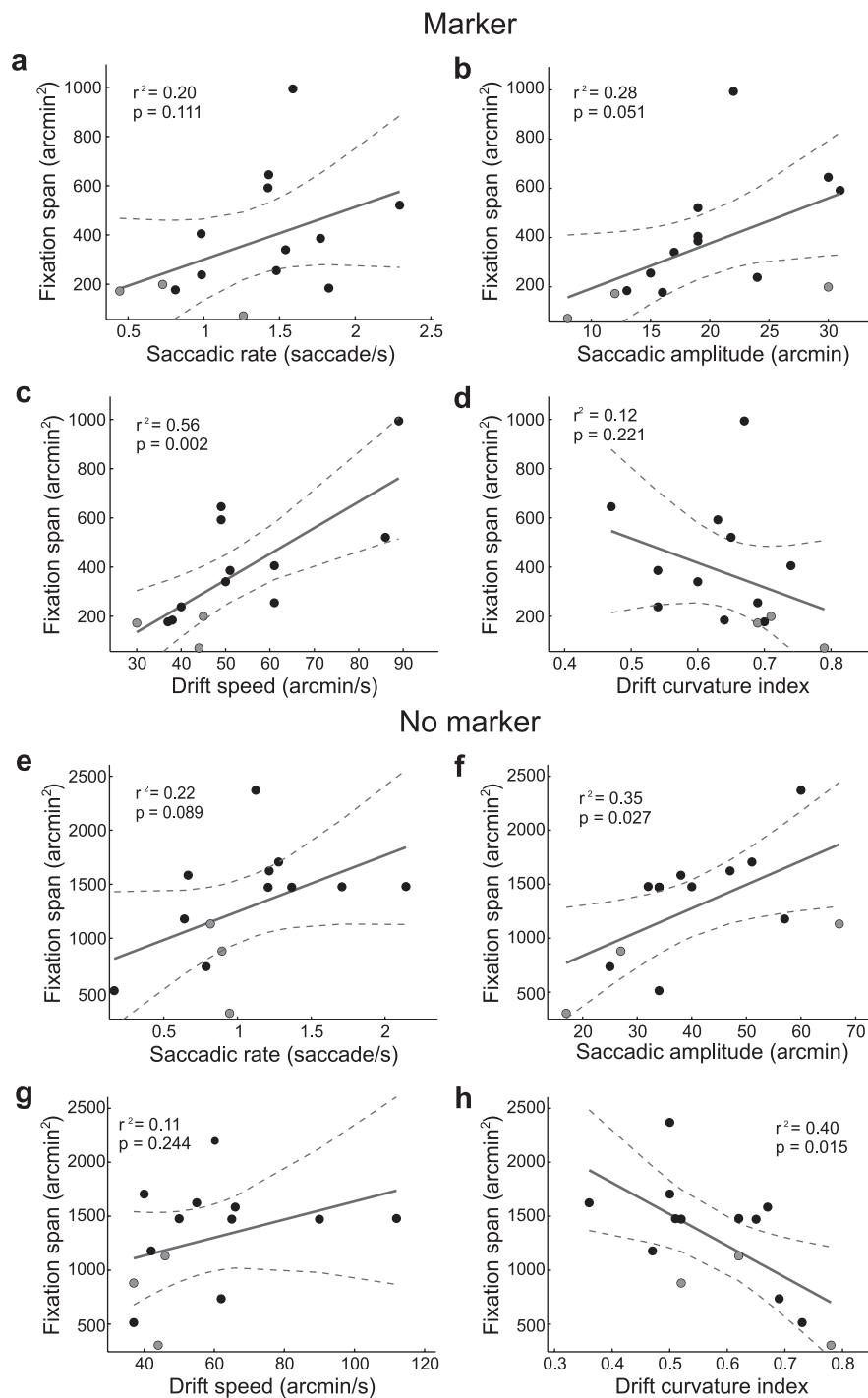


Figure 6. Linear regression between the fixation span and the four oculomotor variables in the marker (a-d) and no-marker condition (e-h). Each dot represents one observer. Experienced subjects are indicated in gray. Solid and dashed lines represent linear regressions and their 95% confidence intervals, respectively. The corresponding values of the coefficient of determination (r^2) and probability (p) are reported in each panel.

of drift velocity underestimate the instantaneous speed of inter-saccadic eye movements. First, these measurements refer to only one component of the velocity vector (typically the horizontal axis) and, therefore, their values are necessarily smaller than the actual modulus of 2D velocity estimated in our study. Second,

velocity estimation requires numerical differentiation of the recorded position traces, a challenging operation susceptible to the influence of noise. In the absence of present-day computational tools, classical studies could only measure average displacements over relatively large intervals, e.g., the average amplitude of the

overall eye displacement in between two successive saccades (Ditchburn, 1973). This approach models ocular drift as uniform linear motion and neglects its curvilinear component. Given that drift tends to change direction frequently, it is not surprising that classical studies severely underestimated the speed of drift. This issue was actually noted by Yarbus (1967), who pointed out that speeds of 30°/s occur frequently when the duration of the considered interval is lowered to 100 or 10 ms. A more recent study that estimated instantaneous speed gave results much closer to the values reported here (Srebro, 1983).

The nonstationary nature of the eye movement traces—with the rapid transitions between saccades and drift—is also a problem in the estimation of drift speed, as filtering may inaccurately spill the high velocities of saccadic intervals over the low velocities of drift periods. For this reason, before performing numerical differentiation, we filtered isolated inter-saccadic periods by means of a local polynomial regression filter (Savitzky & Golay, 1964). This method was preferred over more traditional filters because of its higher stability during the initial and final interval of each drift segment. However, our estimate was not affected by possible saccadic artifacts, as the instantaneous drift speed remained approximately constant throughout the inter-saccadic period. Virtually identical speed estimates were also obtained with a third-order Butterworth filter with 30 Hz cut-off frequency. Use of a higher cutoff frequency would lead to higher estimates of instantaneous speed (e.g., 66°/s at 50 Hz) but would also increase the contribution of noise. Our conservative choice of a 30-Hz cut-off frequency ensured that the noise had little influence in the measurements, an observation supported by the extremely high correlations measured for the drift parameters of individual subjects in the two experimental conditions. Indeed, at 30 Hz, the power of the recorded eye movement traces was more than one order of magnitude higher than the power of noise as measured by means of an artificial eye. Thus, we can safely conclude that the mean speed of eye movement in the inter-saccadic periods is much larger than previously reported in the literature.

Our data provide further support to the proposals that both saccades (Cornsweet, 1956) and drift (Nachmias, 1959) contribute to the maintenance of fixation. The hypothesis that microsaccades play a corrective function during fixation has a long history (Rolfs, 2009). Our data support this proposal in multiple ways. Although individual differences were visible, the characteristics of fixational saccades were highly influenced by the presence/absence of a fixation target. Saccades were (a) larger and (b) less frequent without a fixation marker. Furthermore, (c) their rate was positively correlated with the speed of ocular drift,

and (d) their amplitude negatively correlated with the drift curvature. (e) A saccade also possessed a significant tendency to move the eye in a direction opposite to that of the period of drift which immediately preceded it. (f) This tendency was significantly stronger in the presence of the marker than in its absence. These characteristics are exactly those that one would expect if fixational saccades attempt to correct for displacements caused by ocular drift.

In agreement with previous studies (Nachmias, 1961; Steinman et al., 1973), signs of motor control were also visible in ocular drift, even if they were more subtle than in saccades. Like saccades, also drift was affected by the presence/absence of a fixation target. Drift was slower and more curved in the experienced observers and during fixation on a marker than during fixation on a uniform field. Probability distributions of drift velocity were more symmetrical in the presence of the fixation marker than its absence. Drift also had a tendency to move the eye in the direction opposite to that of the preceding saccade. Although it is clear that drift includes a stochastic component of motion (Kuang et al., 2012), these results support the proposal that drift is, in part, under active control of the oculomotor system (Steinman et al., 1973). Ocular drift is often modeled as some type of random walk (Burak et al., 2010; Engbert et al., 2011; Kuang et al., 2012). Our findings do not exclude Brownian motion as a reasonable working approximation for ocular drift, particularly for brief fixations, but indicate that the model parameters need to change in different viewing conditions (i.e., presence/absence of a clear fixation target).

In all subjects, the accuracy of fixation degraded significantly in the absence of a marker. Since the edges of the monitor were visible, these findings resemble those reported by Sansbury et al. (1973), who showed a gradual decrease in the precision of fixation as the eccentricity of visual stimulation increased. Multiple factors could have contributed to this deterioration in the stability of fixation, including: (a) uncertainty in determining the exact center of the monitor from its edges; and (b) possible errors in judging eye movements from the retinal displacement of peripheral stimuli. Our results do not allow distinction of these possible hypotheses, but the estimation of the central point of a figure is already known to decrease with the eccentricity of stimulation (Klein & Levi, 1987). In addition, the capability of performing precise saccades toward selected points within peripheral shapes (He & Kowler, 1991) seems to speak against errors resulting from possible distortions in the visual field.

In sum, while attempting to maintain fixation, the eyes move by larger amounts and at faster velocities than it is commonly assumed. Our data also show that experiments in which it is necessary to maintain

accurate and prolonged fixation would benefit from screening subjects on the basis of their ocular drift characteristics. In our pool of subjects, the speed of ocular drift was the best predictor of the area covered by the line of sight during fixation on a marker. However, rather than focusing on conditions that minimize retinal image motion, our study emphasizes the need for examining and understanding the influence of a continually moving retinal stimulus on the acquisition and neural encoding of visual information. Under natural viewing conditions, eye movements combine with movements of the head and body to further amplify the fixational motion of the retinal image (Steinman & Collewijn, 1980). The resulting spatiotemporal stimulus may introduce additional challenges in experimental investigations of visual functions, but is the input signal normally received by the retina.

Acknowledgments

This work was supported by National Institutes of Health grant EY18363 and National Science Foundation grants BCS-0719849 and IOS-0843304.

Commercial relationships: none.

Corresponding author: Michele Rucci.

Email: mrucci@bu.edu.

Address: Department of Psychology, Boston University, Boston, Massachusetts, USA.

References

- Ahissar, E., & Arieli, A. (2001). Figuring space by time. *Neuron*, 32(2), 185–201.
- Averill, H. I., & Weymouth, F. W. (1925). Visual perception and the retinal mosaic, II. The influence of eye movements on the displacement threshold. *Journal of Comparative Psychology*, 5(2), 147–176.
- Bennet-Clark, H. C. (1964). The oculomotor response to small target replacements. *Optica Acta (London)*, 11, 301–314.
- Boyce, P. R. (1967). Monocular fixation in human eye movement. *Proceedings of the Royal Society of London. Series B*, 167(8), 293–315.
- Burak, Y., Rokni, U., Meister, M., & Sompolinsky, H. (2010). Bayesian model of dynamic image stabilization in the visual system. *Proceedings of the National Academy of Sciences, USA*, 107, 19525–19530.
- Collewijn, H., & Kowler, E. (2008). The significance of microsaccades for vision and oculomotor control. *Journal of Vision*, 8(14):20, 1–21, <http://www.journalofvision.org/content/8/14/20>, doi:10.1167/8.14.20. [PubMed] [Article]
- Cornsweet, T. N. (1956). Determination of the stimuli for involuntary drifts and saccadic eye movements. *Journal of the Optical Society of America*, 46(11), 987–993.
- Crane, H. D., & Steele, C. (1985). Generation-V dual-Purkinje-image eyetracker. *Applied Optics*, 24(4), 527–537.
- Deubel, H., & Bridgeman, B. (1995). Fourth Purkinje image signals reveal eye-lens deviations and retinal image distortions during saccades. *Vision Research*, 35(4), 529–538.
- Ditchburn, R. W. (1973). *Eye movements and visual perception*. Oxford, UK: Clarendon Press.
- Ditchburn, R. W., & Ginsborg, B. L. (1952). Vision with a stabilized retinal image. *Nature*, 170(4314), 36–37.
- Engbert, R., & Kliegl, R. (2003). Microsaccades uncover the orientation of covert attention. *Vision Research*, 43(9), 1035–1045.
- Engbert, R., Mergenthaler, K., Sinn, P., & Pikovsky, A. (2011). An integrated model of fixational eye movements and microsaccades. *Proceedings of the National Academy of Sciences, USA*, 108(39), E765–E770.
- Fiorentini, A., & Ercoles, A. M. (1966). Involuntary eye movements during attempted monocular fixation. *Atti della Fondazione Giorgio Ronchi*, 21, 199–217.
- Hafed, Z. M., & Clark, J. J. (2002). Microsaccades as an overt measure of covert attention shifts. *Vision Research*, 42(22), 2533–2545.
- He, P. Y., & Kowler, E. (1991). Saccadic localization of eccentric forms. *Journal of the Optical Society of America A*, 8(2), 440–449.
- Klein, S. A., & Levi, D. M. (1987). Position sense of the peripheral retina. *Journal of the Optical Society of America A*, 4(8), 1543–1553.
- Ko, H.-K., Poletti, M., & Rucci, M. (2010). Microsaccades precisely relocate gaze in a high visual acuity task. *Nature Neuroscience*, 13(12), 1549–1553.
- Krauskopf, J., Cornsweet, T. N., & Riggs, L. A. (1960). Analysis of eye movements during monocular and binocular fixation. *Journal of the Optical Society of America*, 50(6), 572–578.
- Kuang, X., Poletti, M., Victor, J. D., & Rucci, M. (2012). Temporal encoding of spatial information

- during active visual fixation. *Current Biology*, 22(6), 510–514.
- Marshall, W. H., & Talbot, S. A. (1942). Recent evidence for neural mechanisms in vision leading to a general theory of sensory acuity. In H. Kluver (Ed.), *Biological symposia—Visual mechanisms, volume 7* (pp. 117–164). Lancaster, PA: Cattel.
- Martinez-Conde, S., Macknik, S. L., Troncoso, X. G., & Dyar, T. A. (2006). Microsaccades counteract visual fading during fixation. *Neuron*, 49(2), 297–305.
- Nachmias, J. (1959). Two-dimensional motion of the retinal image during monocular fixation. *Journal of the Optical Society of America*, 49(9), 901–908.
- Nachmias, J. (1961). Determiners of the drift of the eye during monocular fixation. *Journal of the Optical Society of America*, 51, 761–766.
- Poletti, M., & Rucci, M. (2010). Eye movements under various conditions of image fading. *Journal of Vision*, 10(3):6, 1–18, <http://www.journalofvision.org/content/10/3/6>, doi:10.1167/10.3.6. [PubMed] [Article]
- Rattle, J. D. (1969). Effect of target size on monocular fixation. *Optica Acta*, 16(2), 183–190.
- Riggs, L. A., & Ratliff, F. (1952). The effects of counteracting the normal movements of the eye. *Journal of the Optical Society of America*, 42, 872–873.
- Rolfs, M. (2009). Microsaccades: Small steps on a long way. *Vision Research*, 49(20), 2415–2441.
- Rucci, M., Iovin, R., Poletti, M., & Santini, F. (2007). Miniature eye movements enhance fine spatial detail. *Nature*, 447(7146), 851–854.
- Sansbury, R. V., Skavenski, A. A., Haddad, G. M., & Steinman, R. M. (1973). Normal fixation of eccentric targets. *Journal of the Optical Society of America*, 63(5), 612–614.
- Savitzky, A., & Golay, M. J. E. (1964). Smoothing and differentiation of data by simplified least squares procedures. *Analytical Chemistry*, 36(8), 1627–1639.
- Skavenski, A. A., Hansen, R. M., Steinman, R. M., & Winterson, B. J. (1979). Quality of retinal image stabilization during small natural and artificial body rotations in man. *Vision Research*, 19(6), 675–683.
- Skavenski, A. A., & Steinman, R. M. (1970). Control of eye position in the dark. *Vision Research*, 10(2), 193–203.
- Srebro, R. (1983). Fixation of normal and amblyopic eyes. *Archives of Ophthalmology*, 101(2), 214–217.
- Steinman, R. M. (1965). Effect of target size, luminance, and color on monocular fixation. *Journal of the Optical Society of America*, 55(9), 1158–1165.
- Steinman, R. M., & Collewijn, H. (1980). Binocular retinal image motion during active head rotation. *Vision Research*, 20(5), 415–429.
- Steinman, R. M., Haddad, G. M., Skavenski, A. A., & Wyman, D. (1973). Miniature eye movement. *Science*, 181(4102), 810–819.
- Stevenson, S. B., & Roorda, A. (2005). Correcting for miniature eye movements in high resolution scanning laser ophthalmoscopy. In Manns, F., Soderberg, P. & Ho, A. (Eds.), *Ophthalmic technologies XI*. (pp. 145–151). Bellingham, WA: SPIE Publications.
- Yarbus, A. L. (1967). *Eye movements and vision*. New York: Plenum Press.